Tau pathology and neurochemical changes associated with memory dysfunction in an optimised murine model of global cerebral ischaemia - a potential model for vascular dementia?

Sabah Khan[1], Nadira Y Yuldasheva[1], Trevor FC Batten[1, 2] Alasdair R Pickles[3] Katherine AB Kellett[4] and Sikha Saha[1]

[1]Division of Cardiovascular and Diabetes Research, Leeds Institute of Cardiovascular and Metabolic Medicine, University of Leeds, Leeds, LS2 9JT, UK

[2]Leeds Trinity University, Brownberrie Lane, Horsforth, Leeds LS18 5HD, UK

[3]Faculty of Biological Sciences, University of Leeds, Leeds.LS2 9JT, UK

[4]Division of Neuroscience and Experimental Psychology, Faculty of Biology, Medicine and Health, University of Manchester, Oxford Road, Manchester, M13 9PT, UK

Corresponding author:

Dr Sikha Saha

Division of Cardiovascular and Diabetes Research

Leeds Institute of Cardiovascular and Metabolic Medicine

Worsley Building

University of Leeds

Leeds LS2 9JT

United Kingdom

Phone: +44(0)113-343-4817

Email: s.saha@leeds.ac.uk

Abstract

Cerebral ischemia is known to be a major cause of death and the later development of Alzheimer's disease and vascular dementia. However, ischemia induced cellular damage that initiates these diseases remain poorly understood. This is primarily due to lack of clinically relevant models that are highly reproducible. Here, we have optimised a murine model of global cerebral ischaemia with multiple markers to determine brain pathology, neurochemistry and correlated memory deficits in these animals. Cerebral ischaemia in mice was induced by bilateral common carotid artery occlusion. Following reperfusion, the mice were either fixed with 4% paraformaldehyde or decapitated under anaesthesia. Brains were processed for Western blotting or immunohistochemistry for glial (GLT1) and vesicular (VGluT1, VGluT2) glutamate transporters and paired helical filament (PHF1) tau. The PHF1 tau is the main component of neurofibrillary tangle, which is the pathological hallmarks of Alzheimer's disease and vascular dementia. The novel object recognition behavioural assay was used to investigate the functional cognitive consequences in these mice. The results show consistent and selective neuronal and glial cell changes in the hippocampus and the cortex together with a significant reduction in GLT1 (***P< 0.001), VGluT1 (**P<0.01) and VGluT2 (***P<0.001) expression in the hippocampus in occluded mice as compared to sham-operated animals. These changes are associated with increased PHF1 (***P<0.0001) protein and a significant impairment of performance (*p<0.0006, N=6/group) in the novel object recognition test. This model represents a useful tool for investigating cellular, biochemical and molecular mechanisms of global cerebral ischaemia and may be an ideal preclinical model for vascular dementia.

Key words: Global cerebral ischaemia; Glutamate Transporter; Tau protein; Memory deficit; Vascular Dementia; Glial cells; Hippocampus; Stroke

Introduction

Cerebral ischaemia, which results from stroke, cardiac arrest and cardiac surgery, is one of the most common causes of death and disability worldwide (Flynn et al., 2008; Kim and Johnston 2011). In acute ischemic stroke a blood vessel in the brain gets occluded by thrombosis or embolism, resulting in neuronal damage and death in an area surrounding the occluded vessel (focal ischaemia) whereas global cerebral ischaemia, which is caused by cardiac arrest and cardiac surgery, encompasses wide areas of brain tissue. The pathophysiology resulting from cerebral ischaemia is a leading cause of death and adult disability and a major risk factor for later development of various neurogenerative diseases including Alzheimer's disease and vascular dementia (De la Torre, 2004a; 2004b; Hazell, 2007; Pluta et.al., 2013). A significant proportion (60-90%) of Alzheimer's disease and vascular dementia patients exhibit cerebrovascular pathology including cerebral infarcts and ischaemic lesions leading to more rapid cognitive decline in patients diagnosed with these diseases (Kalaria, 2000). However, cerebral ischaemia induced cellular damage that initiates cerebrovascular pathology and related memory dysfunction remain poorly understood and this has mired the development of new drug treatment strategies. The possible reasons for this failure include lack of a clinically relevant model that is highly reproducible as the pathophysiology of cerebral ischaemia injury in animal models is influenced by numerous factors including the species, type of blood vessels occluded, occlusion period and reperfusion time (Hossmann, 1998).

This study aims to optimise a murine model of global cerebral ischaemia and reperfusion and uses a variety of cellular and neurochemical markers to determine the extent of neuronal and glial cell damage and changes in glutamate transporters in the hippocampus and cortex, as assessed using immunohistochemistry (IHC). Changes in glutamate transporter proteins in the hippocampus were quantified by Western Blotting (WB). Since there is a strong correlation between cerebral ischaemia and the neurodegenerative diseases (Fujii et al., 2016; Kalaria, 2000), we have examined the expression of

hyperphosphorylated tau protein in the hippocampus to determine if ischemic insult in this model results in the development of tau pathology. Hyperphosphorylated tau is known to accumulate as paired helical filament (PHF) which is the main component of neurofibrillary tangle, one of the pathological hallmarks of many neurodegenerative diseases including Alzheimer's disease and vascular dementia (Andorfer et al., 2003; Rissman and Poon 2017). We have also assessed memory correlates of histologically and biochemically determined ischaemic damage in this model. Our hypothesis is that cerebral ischaemia induced cellular damage through alterations in glutamate transporters in the brain lead to neurodegenerative pathology and memory dysfunction.

Materials and Methods:

Animals

All experiments were performed on 10- to 12-week-old (25–30 g) male C57BL/6J mice (Harlan-Olac, Bicester, UK) under appropriate United Kingdom Home Office personal and project licenses and they adhered to the regulations as specified in the U.K. Animals (Scientific Procedures) Act, 1986 and associated guidelines, the European Communities Council Directive of 24 November 1986 (86/609/EEC).

Cerebral ischaemia and reperfusion injury

Cerebral ischaemia was induced in mice (n=48) by transient bilateral common carotid artery occlusion (BCCAO). In brief, under anaesthesia with isoflurane (1-1.5% in oxygen) and intraperitoneal injection of buprenorphine HCL (0.25 mg/ kg), both carotid arteries were isolated through a midline neck incision and occluded with microserrefines. Perfusion was restored by removing the microserrefines after a 10, 15 or 18 min occlusion period (n= 6 per group) and the wound was sutured and anaesthesia discontinued.

Following surgery each mouse was injected intraperitoneally with sterile saline (0.4 ml). For mice in the sham operated group (n=48), the same surgical procedure was performed except that the common carotid arteries were not occluded. Core body temperature was

regulated at 37 ± 0.5°C by a warming plate throughout the procedure and after the operation until the mouse was recovered from anaesthesia. Reperfusion was then allowed for 3 or 7 days, as our pilot study showed no visible ischemic damage following a 1 or 2-day reperfusion. Pilot results also indicated very little ischaemic damage following occlusion of carotid arteries less than 10min even after 7 days reperfusion.

Assessment of neurological deficit

Neurological assessment was performed in BCCAO and sham operated mice by neurological deficit signs including disturbances of consciousness, circling, torsion of the neck and seizure (Yang et al., 1997) i.e., 0, no observable deficit; 1, drowsiness and circling; 2, torsion of the neck and disappearance of the righting reflex; 3, seizure; 4, no spontaneous movement or coma.

Assessment of cerebral ischaemia injury using histochemistry and immunohistochemistry

Following 3 or 7day, BCCAO and sham-operated mice were perfused transcardially with 4% paraformaldehyde in 0.1M phosphate buffer (PB, pH 7.4). Brains were post-fixed overnight and stored in PB at 4°C. Sections cut on a vibrating microtome (Leica Microsystems, Germany) were processed for either cresyl violet staining or IHC according to the methods described in our previous study (Ketheeswaranathan et al., 2011). Antibodies details and dilutions used for IHC are listed in table 1.

Antibody specificity

Antibodies against GLAST (A522) and GLT1 (B12) were prepared by immunising rabbits with C terminal peptide A522–541 (PYQLIAQDNEPEKPVADSET) or N-terminal peptide 12–26 (KVEVRMHDSHLSSE), respectively. These antibodies were raised, purified and extensively characterised as previously described (Lehre and Danbolt 1998 ; Lehre KP et al., 1995). The specificity of polyclonal rabbit antisera raised against VGLUT1 and VGLUT2

and mouse monoclonal antibodies raised against PHF1 were also extensively tested previously [VGLUT1 and -2, (Varoqui et al., 2002) ; PHF1 Tau (Andorfer et al., 2003).

Analysis of histochemical and immunohistochemical data

Cresyl violet stained or immunostained sections were viewed on an AxioImager Z.1 epifluorescence microscope (Carl Zeiss, Welwyn Garden City, UK). Bright field images were captured using a Zeiss AxioVision Imaging System. All images were imported into Adobe Photoshop 7.0 for minor adjustment of brightness and contrast, resizing or cropping and assembling into figures. After lettering, the layers were merged, resolution was adjusted to 500 dpi and the images were saved as TIFF files.

Stereological method for quantification of immunolabelled profiles

The number of NeuN immunoreactive (-IR) neuronal cells and GFAP-IR glial cells per unit volume of tissue in defined brain areas was estimated using a three-dimensional counting method based on the well-established optical dissector method (Williams and Rakie 1988). Areas of the hippocampus and cortical region to be sampled were located by examining immunolabelled sections under bright field light illumination at low magnification (10 objectives). Because most of the mice in our study showed hippocampal and cortical damage in both hemispheres, histological analysis was conducted unilaterally. Analysis was performed at two levels of sectioning from each brain: interaural line (2.34mm to 1.74mm); bregma (1.54mm to 2.06 mm). Images were captured into Axiovision, using the x10 objective. Each captured image corresponded to an area of tissue measuring 450 x 350 um. An acetate sheet with standard unbiased counting frame (Gundersen, 1977), each side equivalent to 200 um at this magnification, was laid over the image on the monitor, to form a counting box for the image. All immunopositive cells falling within the counting frame were marked on the image using the ‘event counting’ facility of the measurement module, and the images were examined to ensure that each cell／nucleus was counted only once. All counts were performed blindly on coded slides by a single observer. Data were analysed using one-

way ANOVA to determine statistical significance and multiple comparison test was used for post-hoc comparisons. $P < 0.05$ was considered statistically significant.

Tissue preparation for Western Blotting

Western blotting analysis were performed on tissue samples from hippocampal regions only. Foo this the mice were killed by decapitation under anaesthesia, brains removed and rapidly frozen on dry ice. Coronal slices of approximately 1mm thickness were cut from the forebrain (over dry ice) with a scalpel blade and then hippocampal tissue samples (25-35 mg) from both sides of the brain were collected at the level of the forebrain corresponding to bregma −0.22 to −2.06mm (Paxinos and Franklin 2014) with 1mm corer under a ×5 dissecting microscope.

Protein extraction

The brain tissue was homogenised using a blunt 20-gauge blunt needle and protein was extracted using SDS-PAGE sample buffer (Tris 500 mM, PH 6.8, glycerol, 100 mM EDTA and 2% SDS). Samples containing total protein were mixed with an equal volume of SDS dissociation buffer (900µl SDS, 100µl beta mecracaptoethanol, 10µl Bromophenol blue solutions) and boiled for 5 min. Protein concentration in samples was measured using the standard BCA method.

Western Blotting

Proteins were resolved by SDS polyacrylamide gel electrophoresis using 10% polyacrylamide gels. Resolved proteins were transferred to Polyvinylidene difluoride membrane (Amersham, GE Healthcare, UK). The membrane was blocked for 1 hr with PBS containing 0.1% (v/v) Tween-20 and 5% (w/v) dried milk powder and incubated at 4^{o} C overnight in primary antibodies against GLT1 (1/3000), VGLUT1 (1/1000), VGLUT2 (1/2000) and PHF1 (1/1000) diluted in PBS- Tween containing 2% (w/v) bovine serum albumin. Horseradish peroxidase-conjugated secondary antibodies, either anti-rabbit or anti-mouse

IgG were used at 1:4000 dilution in PBS-Tween containing 2% (w/v) BSA. Bound antibodies were detected using the enhanced chemiluminescence detection system (Amersham Biosciences, Amersham, UK) and visualised using a Las-3000 Fujifilm imager. Densitometric analysis of blots was performed using image- J software. Data are shown as mean ± SEM, $p<0.001$

Training and assessment in novel object recognition test

Both sham and occluded mice were housed in groups of two. On the day of testing the animals were transferred from the holding room to the room adjacent to the testing area 2 hr prior to testing. Testing comprised of placing animals individually into a cylindrical arena (35 cm diameter) with black walls illuminated from above with a 40 W angle poise lamp to eliminate areas of shadow without creating an overtly bright arena. All animals were handled and habituated to the test arena (with no objects) for at least a week prior to the test to maximise interaction with the objects. The objects utilised for recognition testing were of similar material and texture (plastic) but differed in shape. On day 1 of each experiment (learning phase), the animal was placed in the arena with two identical objects (Familiar: 2 x plastic column, 10 cm high x 2 cm wide constructed from children's building blocks) secured to the floor of the arena and allowed to explore the objects for 2time periods of 10 min, each separated by 5 min. One hour later a novel object (Novel: plastic cross shape, 10 cm x 10 cm) again secured to the floor of the arena was substituted for one of the familiar ones and retention was tested by placing the animal back into the test arena for 5 min (test phase). The amount of time each animal spent exploring the objects was recorded by video camera and scored by an experimenter blind to the experimental condition (occluded vs sham) of each animal. Successful exploration of an object was judged by animal following clearly defined criteria: both forelimbs within a 15cm diameter circle of the object, head orientated directly at the object or physically touching the object with its nose. Scoring was completed by recording the time each animal investigated each object and also the general locomotion behaviour (the animal engaging in general ambulatory activity around the arena).

Differences in object interactions were assessed by calculating the discrimination ration (DR) = Tn/(Tn+Tf) where: Tf = Time with familiar object, Tn= Time with novel object. Non-paired two-way t-tests were utilised to assess any statistical significance of DR and general locomotion between the experimental and sham treated control animals.

Following completion of behavioural tests, mice were euthanized appropriately and brain tissue obtained from the BCCAO mice and sham controls were processed for IHC and WB analysis using specific antibodies as described above and any correlation between cerebral ischaemia induced cellular, neurochemical and behavioural changes was determined.

Results:

Cresyl violet staining

Cresyl violet staining showed ischemic damage, as assessed by chromatolytic changes in the hippocampus (Figure 1A-H) and the cortex (Figure 1J-P) following 15m occlusion and 3day or 7day reperfusion, with a very low mortality (<2%). Cellular damage was also seen in the striatum and thalamus (data not shown). At 24hr reperfusion times very little evidence of degenerative changes was observed. Similarly, 10 min ischaemia produces very little degenerative changes. Ischaemia for 18 min resulted in an adverse outcome (2 deaths and 4 animals requiring immediate euthanasia due to drastic weight loss and impaired movement).

Neuron-specific nuclear protein (NeuN) immunoreactive neurones

NeuN, a marker of mature neurons, was used to identify specifically the extent of neuronal death in the hippocampus (Figures 2A-B) and the cortex (Figures 2C-D). NeuN immunostained sections from BCCAO mice showed that 10 min ischaemia did not induce detectable loss of neurones in the examined area (cortex, hippocampus, stratum and thalamus) even after 7 days reperfusion. The numbers of NeuN-IR nuclei in the cerebral ischaemia group were dramatically decreased in specific regions of the cortex as well as the hippocampus when compared to the sham-operated group. Following 15min ischaemia and

7days reperfusion, cellular death was observed in the hippocampus (figure 2B) and the cortex (figure 2D) and to a lesser degree in the stratum and thalamus (data not shown). Quantitative analysis revealed that the numbers of NeuN positive cells were significantly ($p<0.05$) reduced in the CA1, CA2, CA3 areas of the hippocampus and the somatosensory and the motor areas of the cortex (figure 2E).

Glial fibrillary acidic protein (GFAP) immunoreactivity

Antibody to GFAP, a major protein constituent of glial filaments in differentiated astrocytes was used to identify glial cells. In the sham-operated animals, scattered GFAP-IR cells were distributed throughout the layers of the neocortex and in CA1, CA2, CA3 and dentate gyrus of the hippocampus. Substantial increases in the number and density of the GFAP immunopositive astroglial profiles, including enlarged cytoplasmic processes were found in the hippocampus (figure 3B) and the cortex (figure 3D) of the BCCAO mice following 15 min occlusion and 7 days reperfusion. Quantitative analysis of the GFAP-IR demonstrated that the cerebral ischaemia with 7 days reperfusion significantly increased the GFAP-IR astroglial profiles after the ischemic insult compared to the correspondent regions of the sham operated mice (figure 3E).

Since both histochemical and immunohistochemical studies showed profound disrupted cellular changes in the cortex and the hippocampus visualised using both neuronal and glial markers following 15 min occlusion and 7 days reperfusion, the remainder of the results described below are based on observations in these animals.

Glutamate synthetase (GS) immunoreactivity

Antibodies to GS, the enzyme that converts glutamate to glutamine were used to examine the changes of this enzyme following ischaemia. GS-IR was confined to astrocyte cell bodies and processes and labelling was observed both in BCCAO and in sham operated animals. In sham operated animals, the glial cells had thin regular rims of GS positive

cytoplasm surrounding the nuclei in the hippocampal (figures 4A-B) and cortical regions (figure 4B, D). The extent and intensity of GS-IR both in the hippocampus (B) and the cortex (D) appeared to be changed with increased and redistributed IR profiles in BCCAO mice compared to sham operated group.

Glial cells glutamate transporters (GLT1 and GLAST)

Changes in glial glutamate transporter proteins induced by ischaemia were assessed by IHC using specific antibodies to GLT1 and GLAST. In brains of mice subjected to BCCAO, decreases in GLT1-IR with some irregular, disturbed and distorted morphology of the immunoreactive profiles were observed throughout the hippocampus (figures 4G-H) and the cortex (figures 4I-J) when compared to the sham-operated brains. There appeared to be some redistribution of GLAST-IR profiles within the hippocampus without any noticeable change in the intensity of immunoreactivity. Quantitative WB analysis with the same GLT1 antibodies was used to verify the changes observed using IHC. The results showed a significant decrease of GLT1 protein expression (***P< 0.001, N=6/ group) in the BCCAO brains as compared to the sham-operated brains (figures 4K - L).

Vesicular glutamate transporters (VGLUT-1 and VGLUT-2)

In the BCCAO mice a reduction in both VGLUT1 and VGLUT2 IRs compared to sham operated controls was observed in presumptive nerve terminals in the CA1 and CA2 sub-regions of the hippocampus (figures 5A, B, E, F). Figure 5B and D show the reduced VGLUT1 and VGLUT2 IRs respectively in the hippocampus CA1 areas. In addition, the overall pattern of both VGLUT1 and VGLUT2 IR profiles appeared to be disrupted.

WB analysis for VGLUT1 and VGLUT2 using the same antibodies showed significant reductions in both proteins in the hippocampus (figure 5C VGLUT1; **P<0.01, N=6/group), D VGLUT2; (***P<0.001, N= 6/ group) after cerebral ischaemia as compared to sham operated animals, thereby confirming the IHC results.

PHF1 tau protein

To determine whether the observed immunohistochemical changes in glutamate transporters were associated with development of tau pathology we used anti-PHF1 for immunohistochemical and Western blot analysis. In the sham-operated animals, the pattern of immunostaining for PHF1 was consistent with few labelled profiles. We observed substantially increased intensity of PHF1–immunopositive structures in the hippocampus and cortex in the BCCAO mice. Figures 6A-F shows characteristic staining using the anti-PHF1 in the hippocampus both in sham and cerebral ischaemia animals.

We used the same antibodies for WB analysis to quantify hyperphosphorylated tau protein expression in the hippocampus after ischemic insult. A significant increase of PHF1 (***P<0.0001, t-test N= 6/group) was observed in ischemic hippocampus compared to the sham operated animals (figures 6G, H), consistent with the immunohistochemical observations.

Memory correlates

The same animals, in which glutamate transporter expression and tau pathology were subsequently investigated were subjected to the novel object recognition test, which evaluates non-spatial working memory. Significant impairment of performance in the novel object recognition test (*p<0.0006, N= 6/group) was observed after BCCAO, compared to the sham operated animals (figures 7A, B).

Discussion

The present study is the first systematic study investigating detailed neuronal and glial cell damage and changes in expression of both glial and synaptic glutamate transporter proteins in the cortex and the hippocampus following BCCAO and reperfusion in C57BL/6J mice. It is also the first study to examine the expression of PHF1 tau protein in the hippocampus and correlated memory function in this model.

Several authors have used BCCAO in different strains of mice and reported that C57BL/6 mice subjected to this technique developed selective neuronal death in the hippocampus, cortex and caudate putamen with better survival with this strain (Murakami et al., 1998; Yang et al., 1997). However, very little information is available on detail pathological, biochemical and functional changes in this model. Yang et al (1997) used seven mouse strains in their study and reported that the C57BL/6 strain was most susceptible to BCCAO, due to the poor development of the circle of Willis in this strain.

Transient BCCAO causes selective vulnerability and neuronal death in several regions of the brain. Data from NeuN immunohistochemistry showed a selective loss of neurones in the CA1, CA2 and CA3 areas of the hippocampus and the cortex. Prominent neuronal damage was also observed in the motor, somatosensory and insular cortex. In addition, we investigated the changes in astrocytes following cerebral ischaemia injury. Astrocytes play a major role in the formation and maintenance of the brain cytoarchitecture and in addition to their structural and supportive roles they are involved in controlling synaptic function and maintaining the energy supply to neurones and recycling of neurotransmitters (Papa et al., 2014). Astrocytes, through their end feet, also cover and interact with endothelial cells of brain blood vessels and regulate the blood flow in the brain and control blood brain barrier. Following cerebral ischaemia injury induced by BCCAO, astrocytes processes, as identified by GFAP immunostaining, appeared to be rearranged and have become thicker, which is an indication of reactive gliosis, a reaction with specific structural and functional changes (Burda and Sofroniew , 2014; Papa et al., 2014; Pekny and Nilsson 2005). This may contribute to CNS circuit dysfunction, defining a maladaptive synaptic plasticity in the glial-neuronal network leading to abnormal synaptic transmission (Papa et al., 2014).

The present study also reports an increased expression of GS, an astrocyte-specific enzyme (Shaked et al., 2002) following ischaemic insult. In support of this, it has been reported that activation of cultured cortical astrocytes by glutamate resulted in a prolonged increase of GS

expression in contrast to dramatic loss of glutamate transporter protein levels (Lehmann et al., 2009). However, we could not quantify this due to the lack of antibodies that were suitable for use in WB.

We have evaluated expression of the major glial (GLT1 and GLAST) and synaptic glutamate transporter proteins (VGLUT1 and 2) in the cortex and the hippocampus after transient global ischaemia. When blood flow to the brain is compromised, neurones and glial cells are damaged through excessive activation of glutamate receptors (Flynn et al., 2008, Johnston, 2005). Because astrocytes maintain a high outwardly directed glutamate gradient across the cell membrane, activity of excitatory amino acid transporters in the cell membrane is highly dependent on cellular energy status to ensure efficient uptake of glutamate (Grewer and Rauen 2005). Both GLAST and GLT1 are predominantly expressed by astrocytes (Sims and Robinson 1999) and effectively recycle glutamate back into neurones thereby preventing the build-up of excitotoxic levels of glutamate within the extracellular space (Anderson and Swanson 2000, Danbolt, 2001).

We have earlier reported changes in hippocampal and cortical GLT1 but not GLAST following CI induced by transient middle cerebral artery occlusion in C57BL/6 mice (Ketheeswaranathan et al., 2011). Transient global ischemia has been shown to downregulate glutamate transporter function of astrocytes obtained from the hippocampal CA1 region by decreasing mRNA and protein levels of GLT1 (Yeh et al., 2005). The present study provides further evidence using both IHC and WB that transient CI downregulates GLT1 in the hippocampus. Our IHC study suggested some changes in GLAST-IR in the cortex and hippocampus but we could not quantify this due to the lack of suitable GLAST antibodies for WB.

Our results suggest that expression levels of both VGLUT1 and VGLU2 were reduced significantly in the hippocampus. Changes in VGLUTs were previously reported in brain

ischaemia with variable results. For example, VGLUT2 was downregulated in the CA1 region of the gerbil hippocampus following transient global ischaemia (Iadecola, 2013) and in the rat cerebral cortex and caudate putamen following transient middle cerebral artery occlusion (Sánchez-Mendoza et al., 2010). The later study also reported the reduction of VGLUT1 protein level in the CA1 area of the hippocampus following 7 days after ischaemic insult in rats although these authors observed increased VGLUT1 following 3 days of ischaemia.

Given that we observed a reduction in expression of both vesicular and cell membrane glutamate transporters, together with an apparent upregulation of GS in the hippocampus of mice subjected to BCCAO, we conclude that at least for the hippocampus, excitatory amino acid transporters may be compromised at all points in the glutamate-glutamine cycle. Vesicular glutamate transporters along with specific plasma glutamate transporters and GS may be potential targets for the prevention of excitotoxicity induced by ischemic stroke. Targeting to increase specific glutamate transporter activity in the brain may help to treat vascular diseases in the brain including stroke and vascular dementia.

We have shown a significant increase in the PHF tau protein in the mouse hippocampus following cerebral ischaemic injury. This is in agreement with previously reported data indicating that PHF tau is increased in the hippocampus following BCCAO (Zhu et al., 2017). Tau phosphorylation is a key early event in the pathogenesis of neurodegenerative diseases including AD and vascular dementia. Tau is a microtubule-binding protein that contributes to the stability of microtubules when it is bound to polymerised tubulin. The binding of tau protein to microtubules is reduced by increases in the phosphorylation state of tau and hyperphosphorylation of tau disrupts microtubules and interfere with inter-neuronal organelles leading to neuronal dysfunction, cellular death and memory loss (Clodfelder-Miller et al, 2006; Johnson and Stoothoff 2004; Zhang et al., 2014). Our findings suggest that ischemic neuronal damage and glial cell activation are associated with increased PHF

tau. The exact mechanism involved in the structural cell damage that leads to or is associated with Tau pathology is not known. It is possible that reduced oxygen and glucose availability following chronic cerebral ischaemia insult results in less mitochondrial oxidative phosphorylation and production of optimal ATP levels for energy requiring processes in neurones and glial cells (Kalogeria et al., 2012; Watts et al., 2013).

The results of the novel object recognition (NOR) behavioural assay, utilised to investigate the functional cognitive consequences of the BCCAO in these mice, demonstrated clear changes in novel object discriminatory ability. Experimentally occluded mice showed a significant reduction in the ability to discriminate a novel object which is indicative of memory deficits in this model of spatial and temporal memory (Ennaceur, 2010). This result importantly translates a functional behavioural connection with those pathological changes found in the hippocampus as such behavioural changes are found in the NOR test following hippocampal insults (Clark et al., 2000). Further studies using this model are required to understand the underlying mechanisms of ischemia-induced memory impairment.

In humans, however, it is difficult to distinguish between the cognitive deficits that occur in vascular dementia and Alzheimer's disease due to the similarities in symptom presentation. Nevertheless, the deficits in the mice relate to memory as the novel object recognition task relies on intact memory or previously experienced objects and assesses the behavioural and neural processes mediating storage and/or recall of the features of the previously presented objects (Mumby D.G., 2001). The behavioural results showing a functional memory deficit because of the vascular occlusion in the present study suggests a relationship to vascular dementia.

BCCAO models produce astrocytic and neuronal changes that closely resemble those that have been found in post mortem AD and vascular demented brains (Iadecola 2013; Serrano-Pozo et al., 2011) reinforcing the importance of this model for investigation of

neuronal and glial interaction in the tau pathology and memory dysfunction, raising the possibility of linking cerebral ischaemia and neurodegenerative diseases. The changes in tau protein in the human brain in vascular dementia are, however, not conclusive and changes in tau specifically in the hippocampus, as in our model, have not yet been reported. An increase in the relative amount of PHF-1 and other phosphorylated tau species have been shown in the temporal and frontal cortices of patients with vascular dementia (Mukaetova-Ladinska et al., 2015) and neurofibrillary tangles (NFTs) of tau, including phosphorylated tau species, are reported as a common post-mortem finding in the human vascular dementia brain, although to a lesser degree than that seen in Alzheimer's disease (Day et al., 2015). In addition, truncated tau species have also been identified in vascular dementia and have been suggested to be an early contributor to the formation of neurofibrillary tangles (Day et al., 2015). Changes in CSF total and phospho-tau have also been reported for vascular dementia indicating that changes in tau are significant in the disease (Skillback et al., 2015). While our data demonstrates an increase in PHF tau in our model, whether it is correlated with an increase in amyloid beta peptide remains to be determined.

In conclusion, our results suggest that this optimised murine model of global cerebral ischaemia may be an ideal model to study cerebral ischaemia induced neurodegeneration and astrogliosis and open a new window for treatment of brain ischaemia and related diseases e.g., vascular dementia. Further studies on the interaction of glutamate transporters, GS and tau protein and their behavioural correlates in this model may allow us to find ideal targets to prevent those alterations that ultimately lead to neuronal death and onset of neurovascular disorders with major clinical impact.

Acknowledgements

We acknowledge the financial support of the Yorkshire Alzheimer's Research Trust Yorkshire Network. We sincerely thank Professor Peter Davies, Albert Einstein College of

Medicine, Bronx, NY for antibodies to PHF-1 and Professor Jeffrey D. Erickson LSU Health Sciences Center, New Orleans, LA for antibodies to VGLUT1 and 2.

Declaration of conflicting interests

The author(s) declared no potential conflicts of interest with respect to the research, authorship, and/or publication of this article.

Authors' contributions

SK conducted histological, immunohistochemical and western blot experiments and data analysis. NYY performed all surgical procedures. TFCB supervised some aspects of experimental work and contributed in writing manuscript and production of artwork. ARP conducted behavioral studies and data analysis. KABK helped with initial blot analysis and in writing the WB method and result sections. SS conceived and designed the study, supervised all aspect of experimental work and wrote the manuscript with input from all authors.

References

1. Anderson, C.M., Swanson, R.A., 2000. Astrocyte glutamate transport: review of properties, regulation, and physiological functions. Glia 32, 1-14

2. Andorfer, C., Kress, Y., Espinoza, M., de Silva, R, Tucker, K., Barde Y.A., Duff, K., Davies, P., 2003. Hyperphosphorylation and Aggregation of Tau in Mice Expressing Six Normal Human Tau Isoforms J. Neurochem. 86, 582-591.

3. Burda, J.E., Sofroniew, M.V., 2014. Reactive gliosis and the multicellular response to CNS damage and disease. Neuron 81, 229-48.

4. Clark, R.E., Zola, S.M., Squire, L.R., 2000. Impaired recognition memory in rats after damage to the hippocampus. J Neurosci. 20, 8853–8860.

5. Clodfelder-Miller, B.J., Zmijewska, A.A., Johnson, G.V., Jope, R.S., 2006. Tau is hyperphosphorylated at multiple sites in mouse brain in vivo after streptozotocin-induced insulin deficiency. Diabetes 55, 3320-5.

6. Danbolt, N.C., 2001. Glutamate uptake. Prog. Neurobiol. 65, 1-105.

7. Day, R.J., Mason, M.J., Thomas, C., Poon, W.W., Rohn, T.T., 2015. Caspase-cleaved tau co-localises with early tangle markers in the human vascular dementia brain. PLoS One, DOI:10.1371/journal.pone.0132637

8. De la Torre, J.C., 2004. Is Alzheimer's disease a neurodegenerative or a vascular disorder? Data, dogma, and dialectics. Lancet Neurol. 3, 184-90.

9. De la Torre, J.C., 2004. Alzheimer's disease is a vasocognopathy: a new term to describe its nature. Neurol Res. 26, 517-24.

10. Ennaceur, A., 2010. One-trial object recognition in rats and mice: methodological and theoretical issues. Behav Brain Res. 215, 244–254.

11. Flynn, R.W., MacWalter, R.S., Doney, A.S., 2008. The cost of cerebral ischaemia. Neuropharmacology 55, 250-6.

12. Fujii, H., Takahashi, T., Mukai, T., Tanaka, S., Hosomi, N., Maruyama, H., Sakai, N., Matsumoto, M., 2016. Modifications of tau protein after cerebral ischemia and reperfusion in rats are similar to those occurring in Alzheimer's disease - Hyperphosphorylation and cleavage of 4- and 3-repeat tau. J Cereb Blood Flow Metab 1:271678X16668889.

13. Grewer, C., Rauen, T., 2005. Electrogenic glutamate transporters in the CNS: Molecular mechanism, pre-steady-state kinetics, and their impact on synaptic signaling. J Membr Biol. 203, 1–20.

14. Gundersen, H.J.G., 1977. Notes on the estimation of the numerical density of arbitrary profiles: the edge effect. J Microscope 111, 219–23.

15. Hazell, A.S., 2007. Excitotoxic mechanisms in stroke: an update of concepts and treatment strategies. Neurochem Int. 50, 941-53.

16. Hossmann, K.A., 1998. Experimental models for the investigation of brain ischemia. Cardiovasc Res. 39:106-20.

17. Iadecola, C., 2013. The pathobiology of vascular dementia. Neuron. 80: 844-66.

18. Johnson, G.V., Stoothoff, W.H., 2004. Tau phosphorylation in neuronal cell function and dysfunction. J. Cell Sci . 117, 5721-9.

19. Johnston, M.V., 2005. Excitotoxicity in perinatal brain injury. Brain Pathol. 15, 234-40

20. Kalaria, R.N., 2000. The role of cerebral ischemia in Alzheimer's disease. Neurobiol. Aging 21, 321-30.

21. Kalogeris, T., Baines, C.P., Krenz, M., Korthuis, R.J., 2012. Cell Biology of Ischemia/Reperfusion Injury. Int. Rev. Cell Mol. Biol. 298, 229–317.

22. Ketheeswaranathan, P., Turner, N.A., Spary, E.J., Batten, T.F.C., Saha, S., 2011. Changes in glutamate transporter expression in mouse forebrain areas following focal ischemia.Brain Res 1418, 93-103.

23. Kim, A.S., Johnston, S.C., 2011. Global variation in the relative burden of stroke and ischaemic heart disease. Circulation 124, 314-23.

24. Lehmann, C., Bette, S., Engele, J., 2009. High extracellular glutamate modulates expression of glutamate transporters and glutamine synthetase in cultured astrocytes. Brain Res. 1297, 1-8.

25. Lehre, K.P., Danbolt, N.C., 1998. The number of glutamate transporter subtype molecules at glutamatergic synapses: chemical and stereological quantification in young adult rat brain. J. Neurosci. 18, 8751-7.

26. Lehre, K.P., Levy, L.M., Ottersen,. OP., Storm-Mathisen, J., Danbolt, N.C., 1995. Differential expression of two glial glutamate transporters in the rat brain: quantitative and immunocytochemical observations J. Neurosci. 15, 1835-1853

27. Mukaetova-Ladinska, E.B., Abdel-All, Z., Mugica, E.S., Li, M., Craggs, L.J., Oakley, A..E., Honer, W.G., Kalaria, R.N., 2015. Tau proteins in the temporal and frontal cortices in patients with vascular dementia. J..Neuropath. Expt. Neurol. 74, 148-157

28. Mumby, D.G., 2001. Perspectives on object-recognition memory following hippocampal damage: lessons from studies in rats. Behav Brain Res. 127,159-81.

29. Murakami, K., Kondo, T., Kawase, M., Chan, P.H., 1998. The development of a new mouse model of global ischemia: focus on the relationships between ischemia

duration, anesthesia, cerebral vasculature, and neuronal injury following global ischemia in mice. Brain Res. 780, 304–10.

30. Nour, M., Scalzo, F., Liebeskind, D.S., 2013. Ischemia-Reperfusion Injury in Stroke. Interv Neurol. 1, 185–199.

31. Pan, J., Konstas, A.A., Bateman, B., Ortolano, G.A., Pile-Spellman, J., 2007. Reperfusion injury following cerebral ischemia: pathophysiology, MR imaging, and potential therapies Neuroradiol. 49, 93–102.

32. Papa, M., Luca, C.D., Petta, F., Alberghina, L., Cirillo, G., 2014. Astrocytes-neurone interplay in maladaptive plasticity. Neurosci. Biobehav. Rev. 42, 35-54.

33. Paxinos G, Franklin KBJ (2014) The Mouse Brain in Stereotaxic Coordinates (4th edition). Academic Press, San Diego

34. Pekny, M., Nilsson, M., 2005. Astrocyte activation and reactive gliosis. Glia 50, 427-34.

35. Pluta, R., Jabłoński, M., Ułamek-Kozioł, M., Kocki, J., Brzozowska, J., Januszewski, S., et al., 2013. Sporadic Alzheimer's disease begins as episodes of brain ischemia and ischemically dysregulated Alzheimer's disease genes. Mol. Neurobiol. 48, 500-15

36. Rissman, R.A., Poon, W.W., 2017. Blurton-Jones M, et al. Caspase-cleavage of tau is an early event in Alzheimer disease tangle pathology, The Journal of Clinical Investigation. 114, 121-130

37. Sánchez-Mendoza, E., Burguete, M.C., Castelló-Ruiz, M., González, M.P., Roncero, C., Salom, J.B., Arce, C., Cañadas, S., Torregrosa, G., Alborch, E., Oset-Gasque, M.J., 2010. Transient focal cerebral ischemia significantly alters not only EAATs but also VGLUTs expression in rats: relevance of changes in reactive astroglia. J. Neurochem. 113, 1343-55.

38. Sanderson, T.H., Reynolds, C.A., Kumar, R., Przyklenk, K., Huttemann, M., 2013. Molecular mechanisms of ischemia-reperfusion injury in brain: pivotal role of the mitochondrial membrane potential in reactive oxygen species generation. Mol Neurobiol. 47, 9-23.

39. Serrano-Poz,o A,. Frosch, M.P., Masliah, E., Hyman, B.T., 2011. Neuropathological Alterations in Alzheimer Disease. Cold Spring Harb Perspect Med. 1, a006189. doi: 10.1101/cshperspect.a006189.

40. Shaked, I., Ben-Dror, I., Vardimon, L., 2002. Glutamine synthetase enhances the clearance of extracellular glutamate by the neural retina. J Neurochem. 83, 574-80.

41. Sims, K.D., Robinson, M.B., 1999. Expression patterns and regulation of glutamate transporters in the developing and adult nervous system. Crit. Rev. Neurobiol. 13, 169-97.

42. Skillbäck, T., Farahmand, B.Y., Rosén, C., Mattsson, N., Nägga, K., Kilander, L., Religa, D., Wimo, A., Winblad, B., Schott, J.M., Blennow, K., Eriksdotter, M., Zetterberg, H., 2015. Cerebrospinal fluid tau and amyloid-β1-42 in patients with dementia. Brain 138, 2716-2731

43. Varoqui, H., Schäfer, M.K.H., Zhu, H., Weihe, E., Erickson, J.D., 2002. Identification of the differentiation-associated Na^+/Pi transporter as a novel vesicular glutamate transporter expressed in a distinct set of glutamatergic synapses. J. Neurosci. 22, 142-155.

44. Watts, L.T., Lloyd, R., Garling, R.J., Duong, T., 2013. Stroke Neuroprotection: Targeting Mitochondria. Brain Sci 3, 540–560.

45. Williams, R.W., Rakie, P., 1988. Three-dimensional counting: An accurate and direct method to estimate numbers of cells in sectioned material. J. Com. Neurol. 278, 344 – 352

46. Yang, G., Kitagawa, K., Matsushita, K., Mabuchi, T., Yagita, Y., Yanagihara, T., Matsumoto, M., 1997. C57BL/6 strain is most susceptible to cerebral ischemia following bilateral common carotid occlusion among seven mouse strains: selective neuronal death in the murine transient forebrain ischemia. Brain Res. 752, 209-18.

47. Yeh, T.H., Hwang, H.M., Chen, J.J., Wu, T., Li, A.H., Wang, H.L., 2005. Glutamate transporter function of rat hippocampal astrocytes is impaired following the global ischemia. Neurobiol Dis. 18, 476-83.

48. Zhang, C.E., Yang, X., Li, L., Sui, X., Tian, Q., Wei, W., Wang, J., Liu, G., 2014. Hypoxia-induced tau phosphorylation and memory deficit in rats. Neurodegener. Dis.14, 107-16.

49. Zhu, Y., Zhang, Q., Zhang, W., Li, N., Dai, Y., Tu., J., Yang, F., Brann, D.W., Wang, R., 2017. Protective effect of 17β-estradiol upon hippocampal spine density and

cognitive function in an animal model of vascular dementia, Scientific Reports 7, 42660, DOI: 10.1038/srep42660

Figure legends:

Figure 1: Coronal sections through the hippocampus (A-H) and cerebral cortex (J-P) stained with Cresyl Violet in BCCAO and sham-operated mice. A & B show low power images of the hippocampus in sham-operated (A) and BCCAO (B) mice. Panels C-D, E-F and G-H show higher magnification images from, respectively CA1, CA2 and CA3 areas. Note the disrupted acidophilic neurones with evidence of small pyknotic cell nuclei in images D, F and H from BCCAO mice. I-P: Similar changes are observed in the motor cortex (I-L) and somatosensory cortex (M-P).

Scale bars: A-B, I-J, M-N, 200µm; C-H, 50µm; K-L, O-P 25µm.

Figure 2: NeuN-IR neurones on forebrain sections from sham-operated (A, C) and BCCAO (B, D) mice. In both the hippocampal CA1 (B) and the motor cortex (D) a disruption and loss of neurones with ischaemia is apparent. Scale bars 50µm.

E: Quantitative analysis shows significant differences ($P<0.001$ ***, N= 6/group) in the number of NeuN-positive neurones between sham-operated and BCCAO mice in the somatosensory cortex (SS1) motor cortex (M1 and M2) and hippocampal CA1, CA2 and CA3 areas.

Figure 3: GFAP-IR astrocytes on forebrain sections from sham-operated (A, C) and BCCAO (B, D) mice. In both the hippocampal CA1 (B) and the somatosensory cortex (D) an increase labelling of astrocytic processes indicative of reactive gliosis is apparent. Scale bars 50µm.

E: Quantitative analysis shows significant increases ($P<0.0001$ *** and N=6/group) in the number of GFAP labelled astrocyte profiles in BCCAO mice compared to sham in the somatosensory cortex (SS1) motor cortex (M1 and M2) and hippocampal CA1, CA2 and CA3.

Figure 4: Immunolabelling of GS (A-D), GLAST (E-F) and GLT1 (G-J) in forebrain sections from sham-operated and BCCAO mice. Scale bars 50 µm.

GS-IR in hippocampus CA1 appears upregulated in cell processes in BCCAO (B) as compared to sham-operated (A) brains. Similarly, GS expression in the motor cortex (D) appears upregulated in BCCAO mice.

E-F: The distribution of GLAST-IR in the hippocampus appears similar in both sham-operated (E) and BCCAO (F) mice.

G-H; I-J: GLT1-IR is reduced in BCCAO compared to sham-operated mice in both hippocampus CA1 (G-H) and somatosensory cortex (I-J).

K-L: WB analysis of GLT1 expression in hippocampus of sham-operated and BCCAO mice. K, band of approximately 60 KDa is greatly reduced in BCCAO compared to sham. L, quantitative analysis of GLT1 band density relative to ß-actin shows a significantly reduced expression in BCCAO mice (***P< 0.001, N=6/group).

Figure 5: VGLUT1 and VGLUT2-IRs in the hippocampus of sham-operated and BCCAO mice. Scale bars 50 µm.

A-D: The distribution of VGLUT1-IR puncta in CA1 appears reduced and disrupted in BCCAO (B) compared to sham (A). WB (C) reveals attenuated expression of VGLUT1 in the hippocampus after BCCAO as evidenced by the reduction in intensity of the band at approximately 47.5 KDa. Quantitative analysis (D) shows a significant reduction (**P<0.01, N=6/group) in VGLUT1 expression in BCCAO mice.

E-H: Similarly, the VGLUT2-IR in CA1 show disrupted organisation in BCCAO (F) compared to sham (E). WB (G) and quantitative analysis (H) confirm significantly reduced (***P<0.001, N= 6/group) expression of VGLUT2 in BCCAO mice.

Figure 6: Evidence for the development of tauopathy in the ischemic brain identified by antibody to PHF1. Prominent PHF1-IRs are found scattered throughout the hippocampus in

BCCAO mice (B, D), but this is not evident in sham-operated mice (A, C). Similarly, dense aggregations of PHF-1 IR are seen in the ischemic cortex in BCCAO mice (F) as compared to sham €. Scale bars 100 µm (A-B); 50 µm (C-F).

G: WB demonstrates a lack of PHF1 signal in the hippocampus of sham-operated mice. H: Densitometric quantitative analysis shows a very significant increase (***P<0.0001, t-test N= 6/group) in hyperphosphorylated tau with ischaemia in hippocampus of BCCAO mice.

Figure 7: Memory function comparing sham-operated mice (Sham) vs mice with BCCAO. Discrimination ratio: (DR) = Tn/(Tn+Tf); Tf = Time with familiar object, Tn= Time with novel object. Significant impairment of performance in the novel object recognition test (*p<0.0006, N= 6/group) is observed in BCCAO mice compared to the sham-operated animals (B).

Table 1. Sources and Specifics of Antisera

Primary/ secondary Antisera	Species raised in	Optimal dilution for IHC	Optimal dilution for WB	Raised and characterised by
GLT-1 (B12)	Rabbit	1/2000	1/3000	NC Danbolt (Lehre et al., 1995; Lehre and Danbolt, 1998)
GLAST (A522)	Rabbit	1/2000	-	NC Danbolt (Lehre et al., 1995; Lehre and Danbolt, 1998)
V-GluT-1	Rabbit	1/4000	1/1000	Jeffrey D. Erickson (Varoqui et al., 2002)
V-GluT-2	Rabbit	1/4000	1/2000	Jeffrey D. Erickson (Varoqui et al., 2002)
PHF Tau	Mouse	1/1000	1/1000	Peter Davies Andorfer et al., 2003)
NeuN	Mouse	1/5000	-	Millipore, UK
GFAP	Mouse	1/1000	-	Sigma, UK
GS	Mouse	1/1000	-	Sigma, UK
Biotinylated anti-mouse IgG	Donkey	1/500	1/4000	Jackson, Immunoresearch, UK
Biotinylated anti-mouse IgG	Donkey	1/500	1/4000	Jackson Immunoresearch, UK

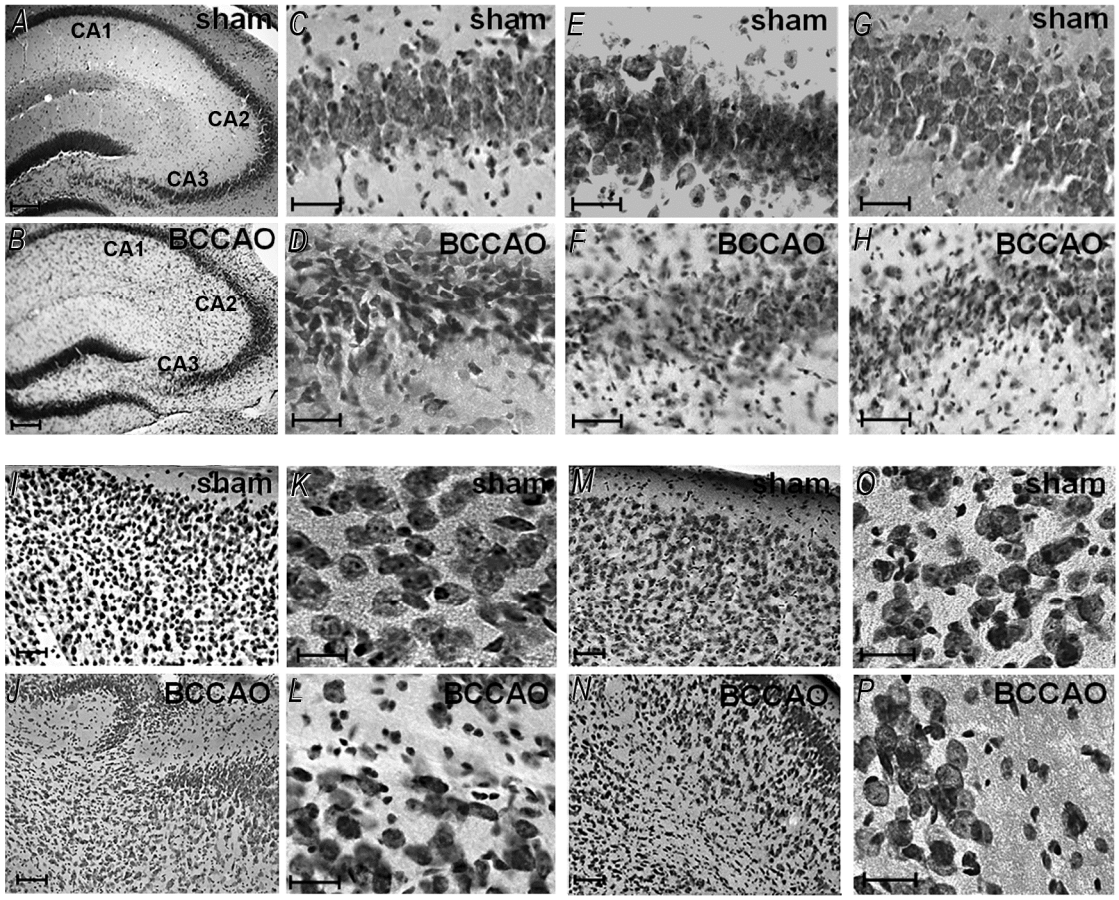
A
sham
CA1
CA2
CA3
C
sham
E
sham
G
sham
B
BCCAO
CA1
CA2
CA3
D
BCCAO
F
BCCAO
H
BCCAO
I
sham
K
sham
M
sham
O
sham
J
BCCAO
L
BCCAO
N
BCCAO
P
BCCAO

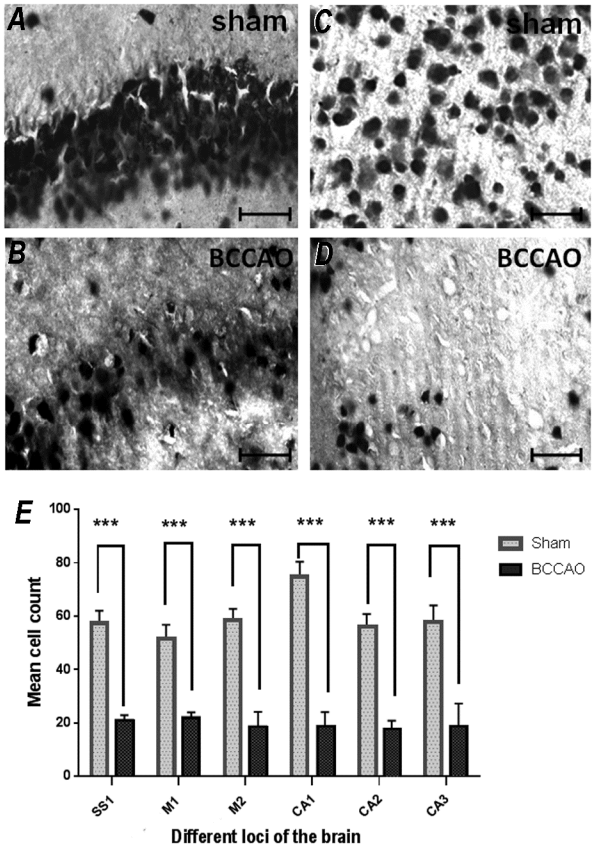
A
sham
C
sham
B
BCCAO
D
BCCAO
E
***
***
***
***
***
***
Sham
BCCAO
Mean cell count
100
80
60
40
20
0
SS1
M1
M2
CA1
CA2
CA3
Different loci of the brain

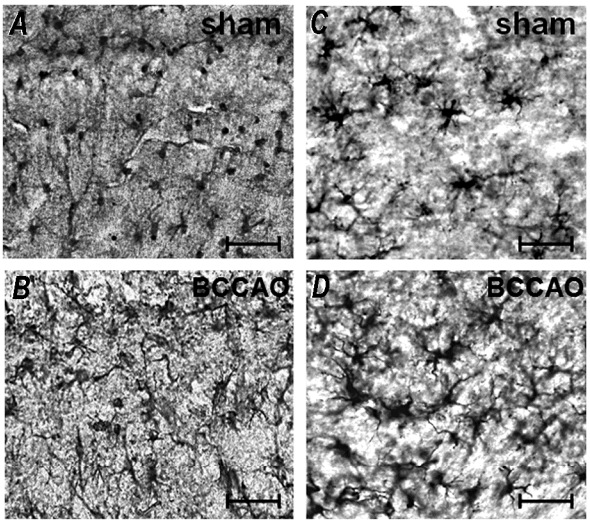
A
sham
C
sham
B
BCCAO
D
BCCAO

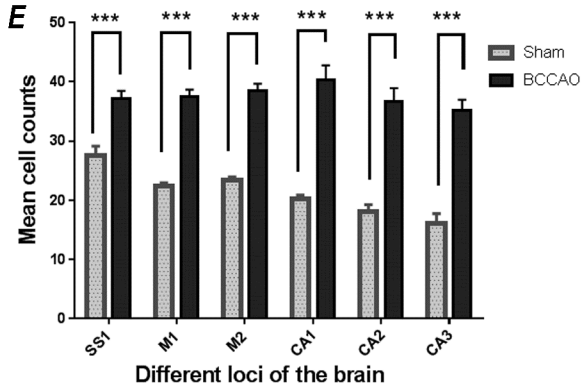
E
***
***
***
***
***
***
Sham
BCCAO
Mean cell counts
50
40
30
20
10
0
SS1
M1
M2
CA1
CA2
CA3
Different loci of the brain

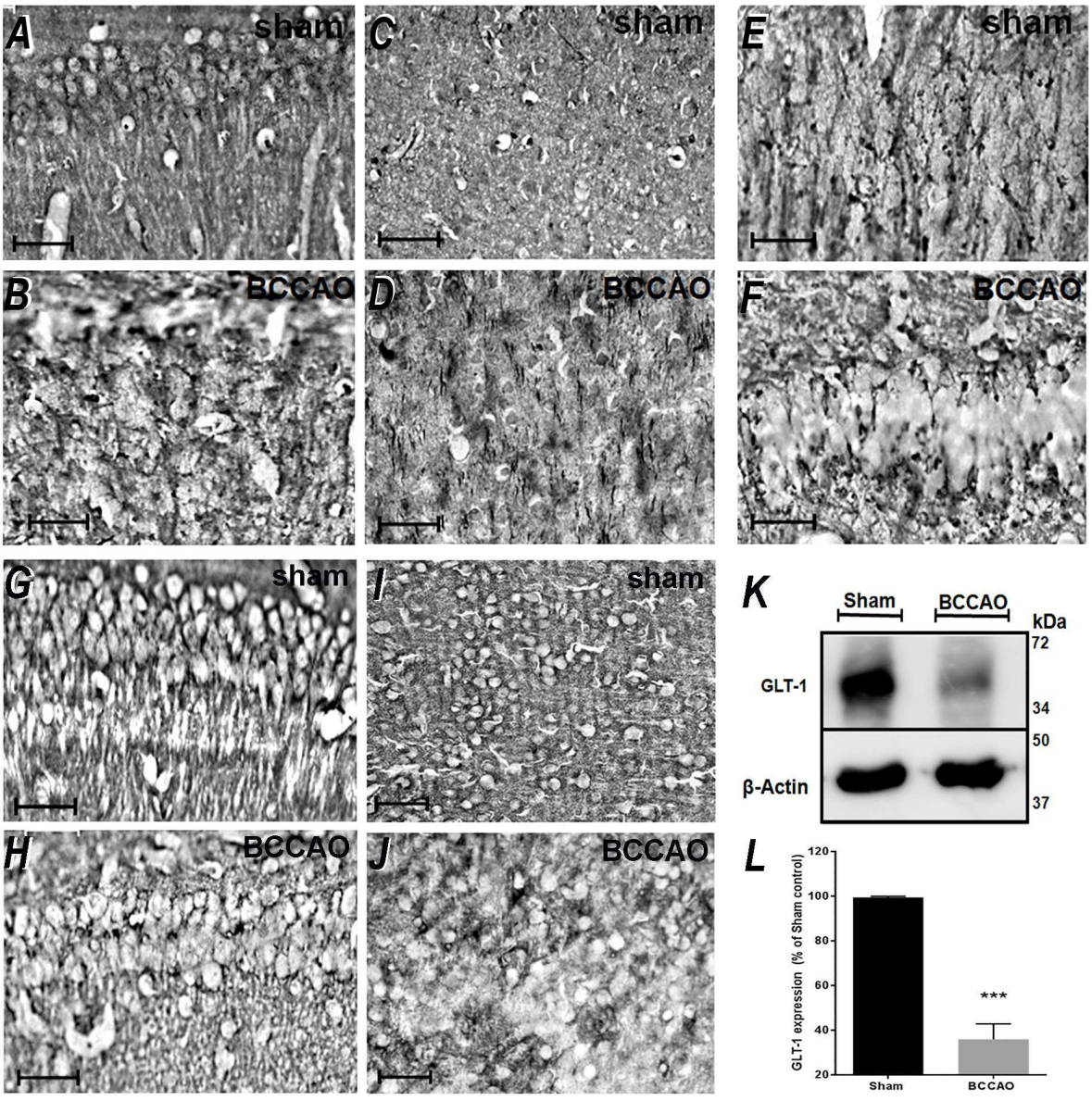
A
sham
C
sham
E
sham
B
BCCAO
D
BCCAO
F
BCCAO
G
sham
I
sham
K
Sham
BCCAO
kDa
72
GLT-1
34
50
β-Actin
37
H
BCCAO
J
BCCAO
L
GLT-1 expression (% of Sham control)
120
100
80
60
40
20
***
Sham
BCCAO

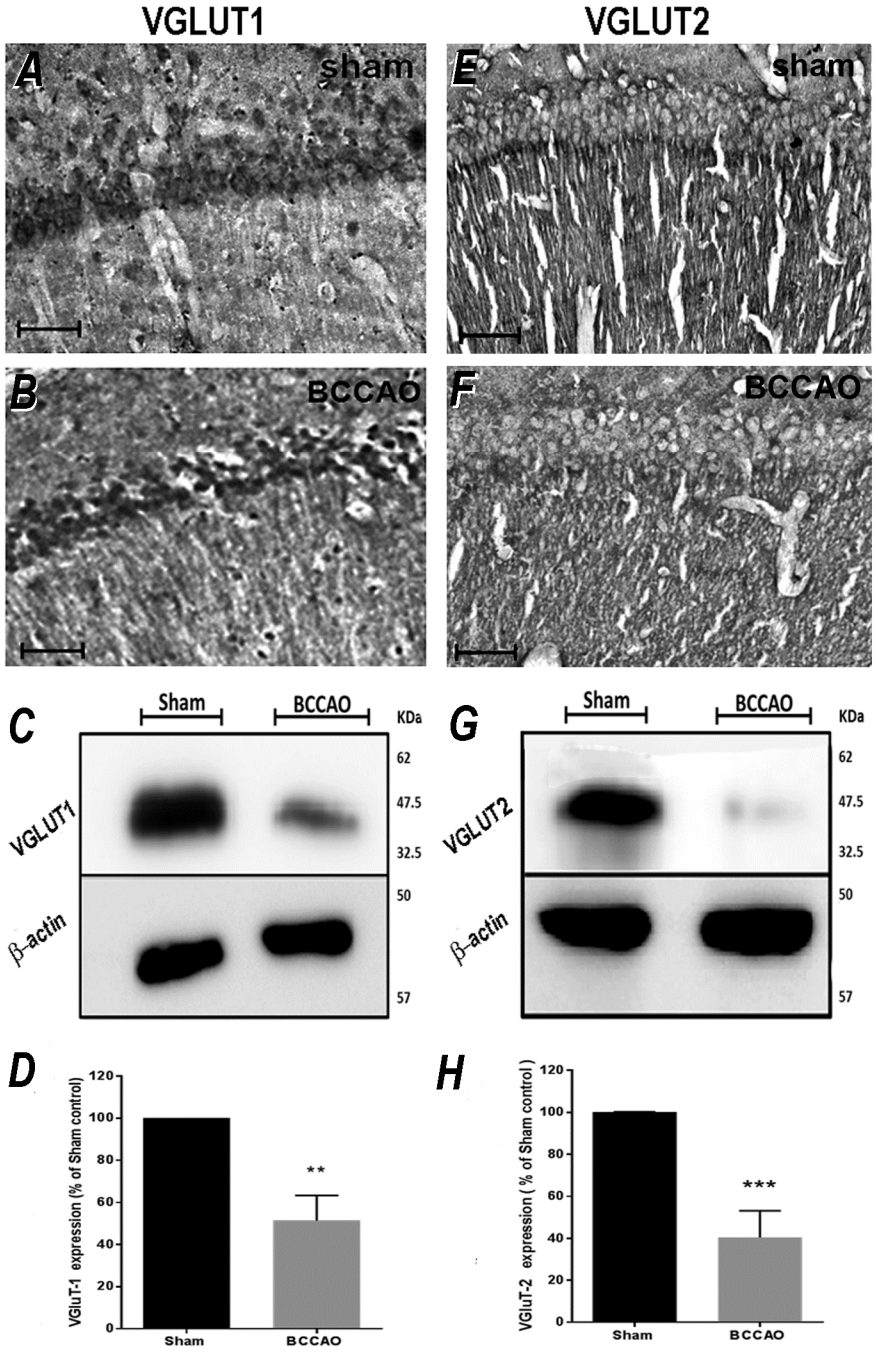
VGLUT1
VGLUT2
A
sham
E
sham
B
BCCAO
F
BCCAO
C
Sham
BCCAO
KDa
62
47.5
32.5
50
57
VGLUT1
β-actin
G
Sham
BCCAO
KDa
62
47.5
32.5
50
57
VGLUT2
β-actin
D
VGluT-1 expression (% of Sham control)
120
100
80
60
40
20
0
**
Sham
BCCAO
H
VGluT-2 expression (% of Sham control)
120
100
80
60
40
20
0
***
Sham
BCCAO

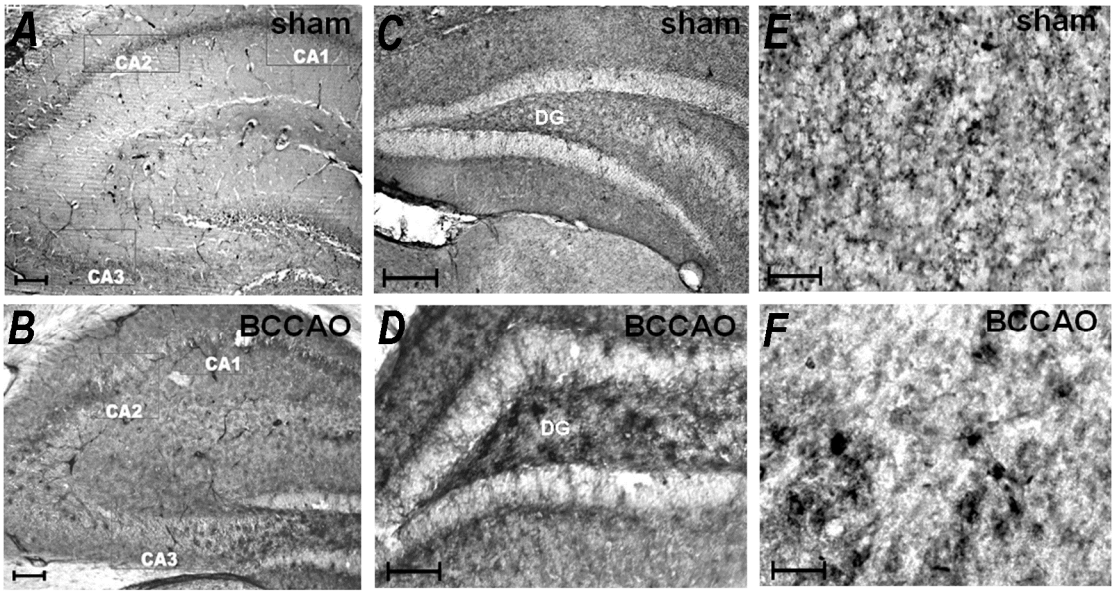
A
sham
CA2
CA1
CA3
C
sham
DG
E
sham
B
BCCAO
CA1
CA2
CA3
D
BCCAO
DG
F
BCCAO

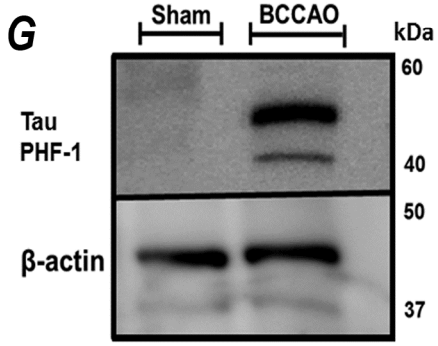
G
Sham
BCCAO
kDa
Tau
PHF-1
β-actin
60
40
50
37

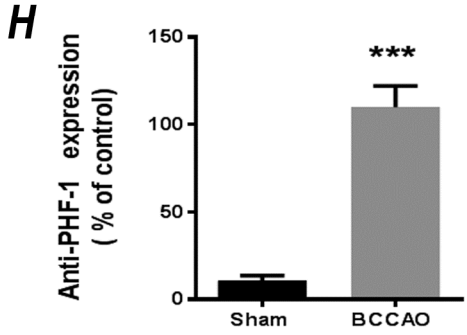
H
Anti-PHF-1 expression
(% of control)
150
100
50
0
***
Sham
BCCAO

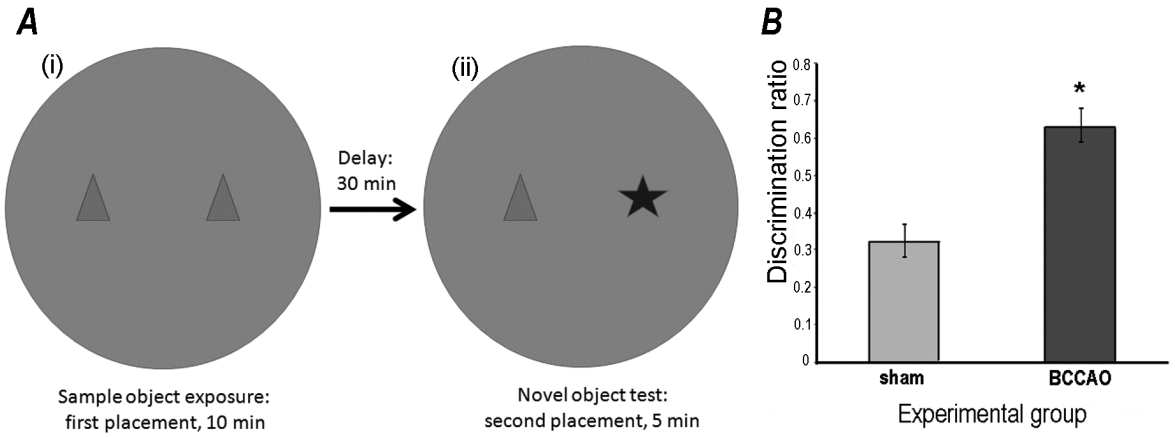
A
(i)
(ii)
Delay:
30 min
Sample object exposure:
first placement, 10 min
Novel object test:
second placement, 5 min
B
Discrimination ratio
0.8
0.7
0.6
0.5
0.4
0.3
0.2
0.1
0
*
sham
BCCAO
Experimental group

Highlights

1. The present study optimised a murine model of global cerebral ischaemia which show consistent and selective neuronal and glial cell changes in the hippocampus and the cortex
2. There are significant reduction in GLT1 (***P< 0.001), VGluT1 (**P<0.01) and VGluT2 (***P<0.001) expressions in the hippocampus in occluded mice as compared to sham-operated animals.
3. There is a significant increase in PHF1 (***P<0.0001) protein in the hippocampus with a significant impairment of performance (*p<0.0006, N=6/group) in the novel object recognition test in ischaemic mice as compared to sham-operated mice.
4. This model represents a useful tool for investigating cellular, biochemical and molecular mechanisms of global cerebral ischaemia and an ideal model for studying cerebral ischaemia induced vascular dementia.